

(微視的) チャネル結合法を用いた直接核反応の研究

北大情報基盤センター
平林義治

○入射粒子-標的核系の直接反応（弹性・非弹性散乱、分解反応）

→ Coupled-Channels method

○核（入射核、標的核）の内部波動関数を（なるべく）微視的に

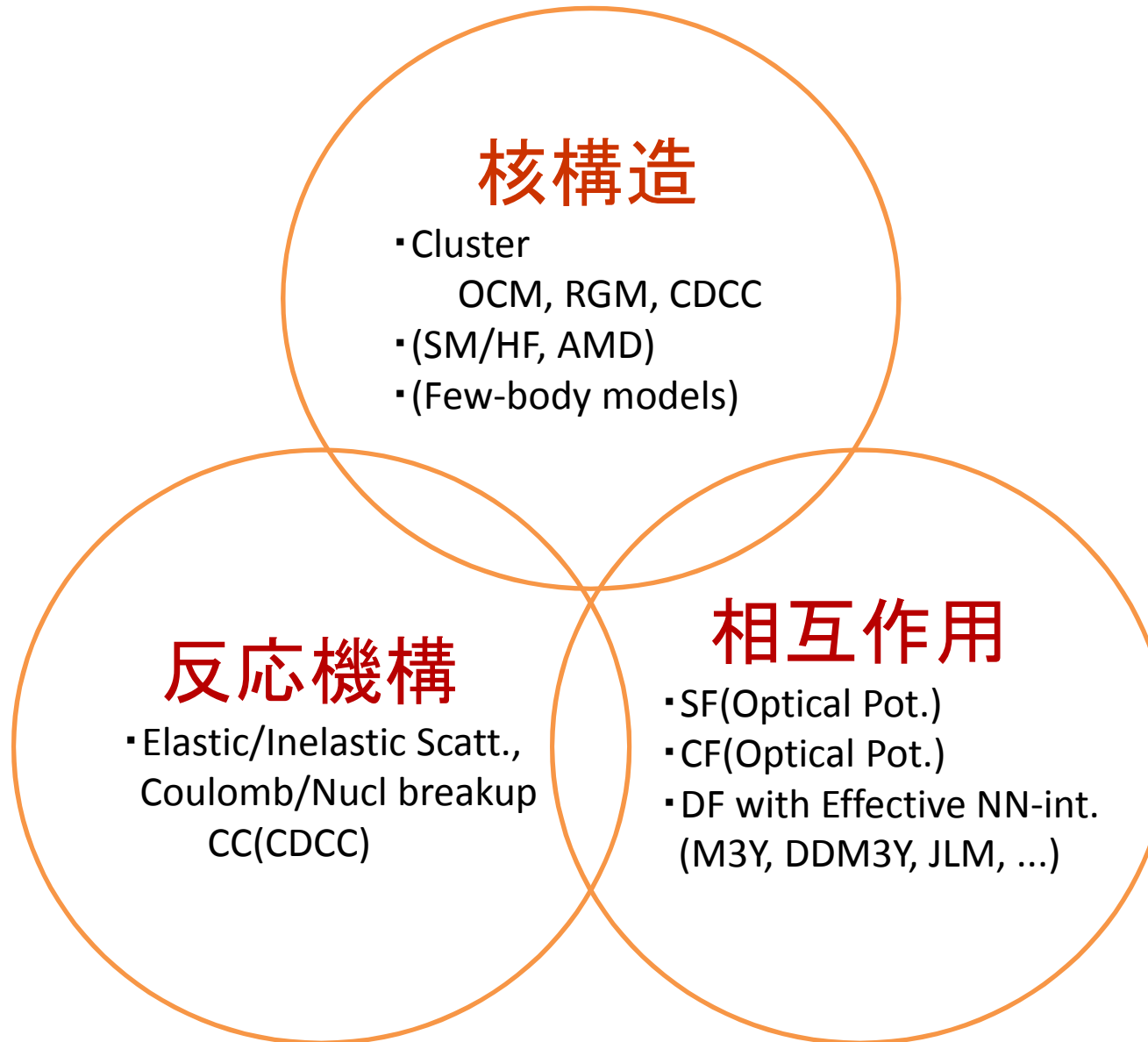
→ (CC)OCM, RGM, CDCC

○反応系（入射核+標的核間）の相互作用

核力・Coulomb力の diagonal, off-diagonal(coupling) potential

→ Folding type (SF, CF, DF(M3Y, DDM3Y, JLM, ...))

○微視的チャネル結合法



○Coupled-Channels Equations

入射粒子--標的核相對波動関数

$$(K_\beta + V_{\beta\beta}(r) - E_\beta)\chi_\beta^{(+)}(r) = - \sum_{\gamma \neq \beta}^N V_{\beta\gamma}(r)\chi_\gamma^{(+)}(r)$$

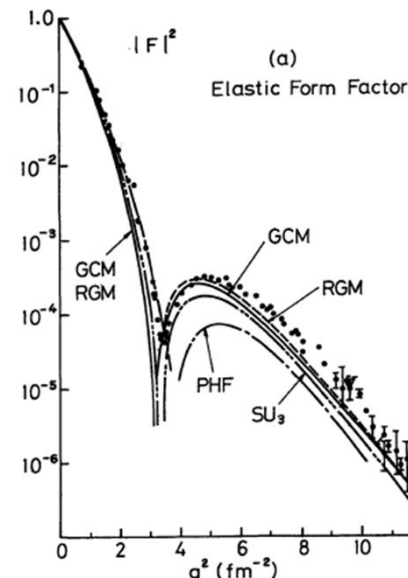
$$(\beta = 1, 2, 3, \dots, N)$$

$$V_{\beta\gamma}(r) \equiv \langle \Phi_\beta(\xi) | V | \Phi_\gamma(\xi) \rangle_\xi$$

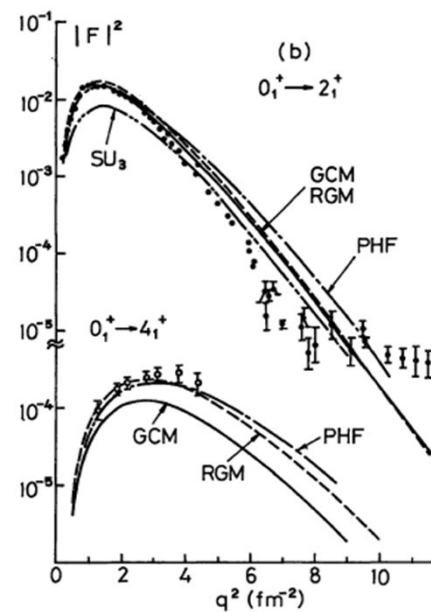
入射粒子--標的核間相互作用
(Folding type)

核の内部対波動関数

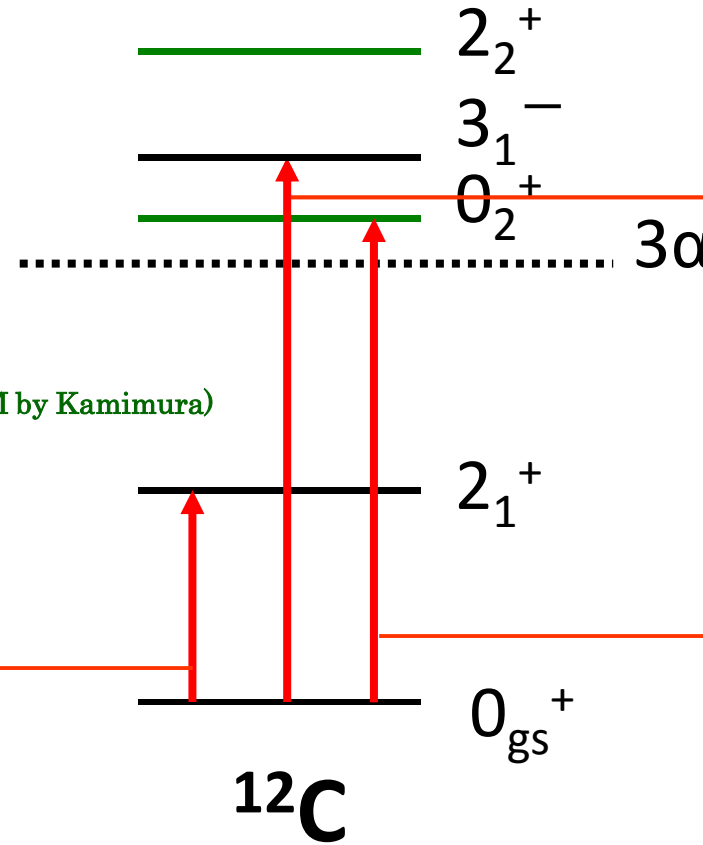
○ 核（入射粒子、標的核）の微視的波動関数（例： ^{12}C ）



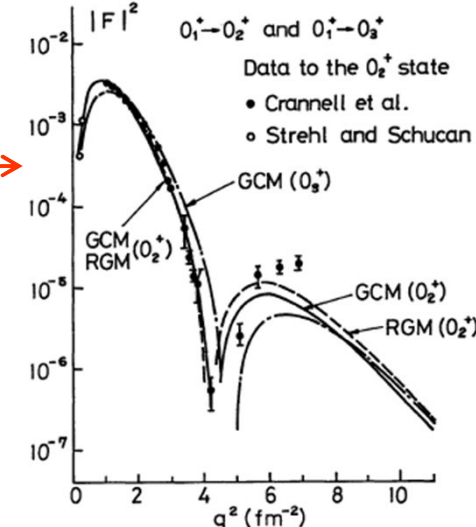
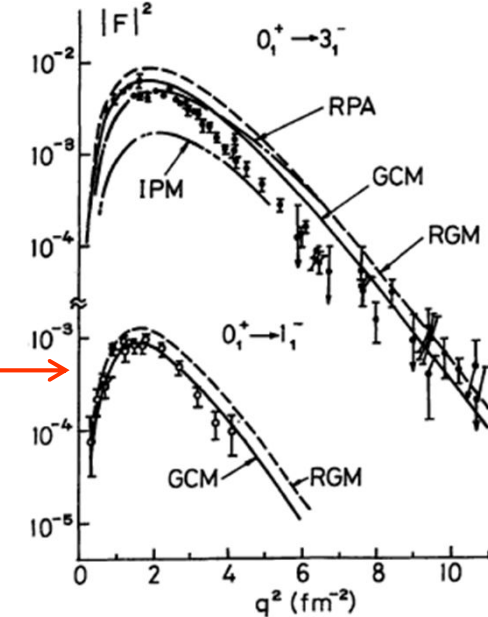
PTP Suppl. 68, '80 (GCM by Uegaki, RGM by Kamimura)



電子散乱形状因子の実験・理論比較

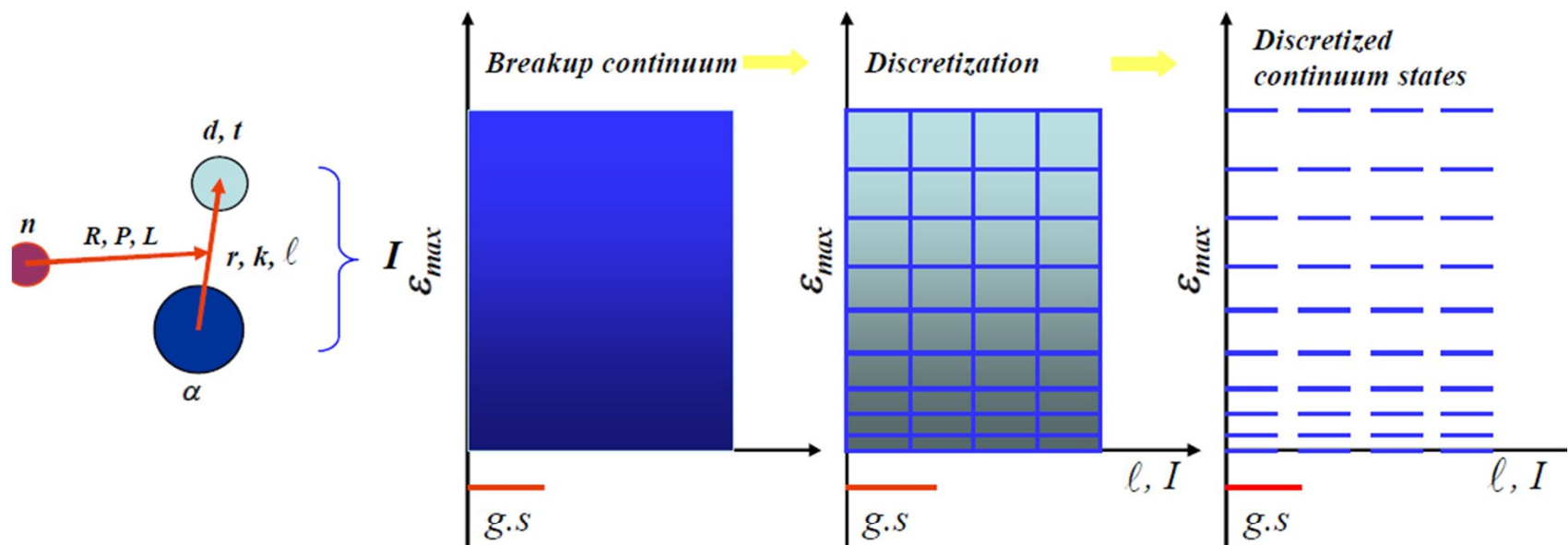


構造遷移が正しく記述されていることが非常に重要



○ 核の微視的波動関数（例：CDCC）

The Method of CDCC in $^{6,7}\text{Li}$



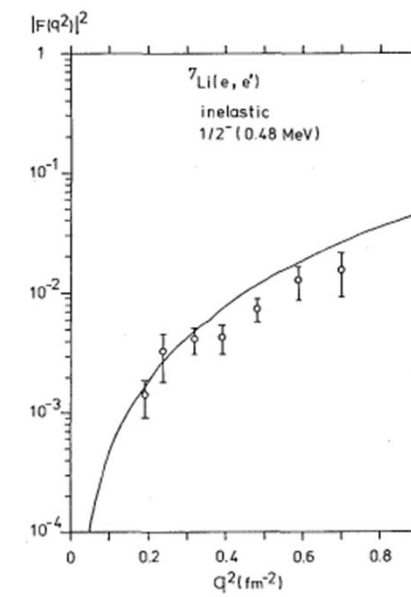
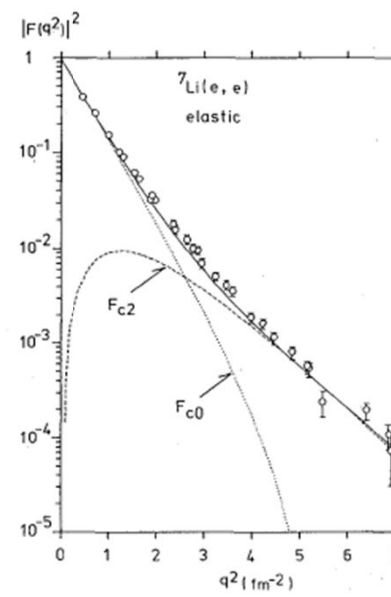
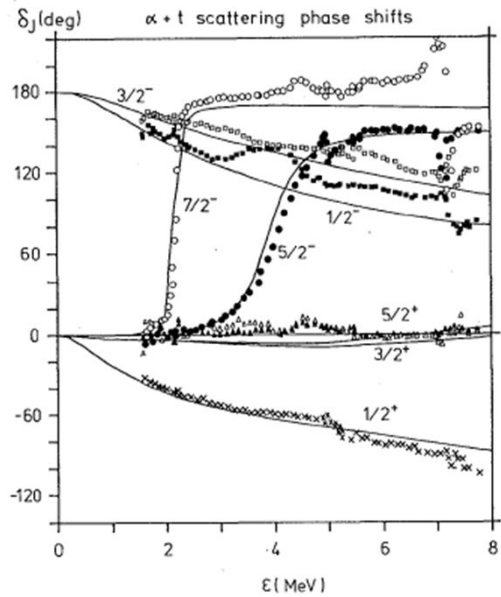
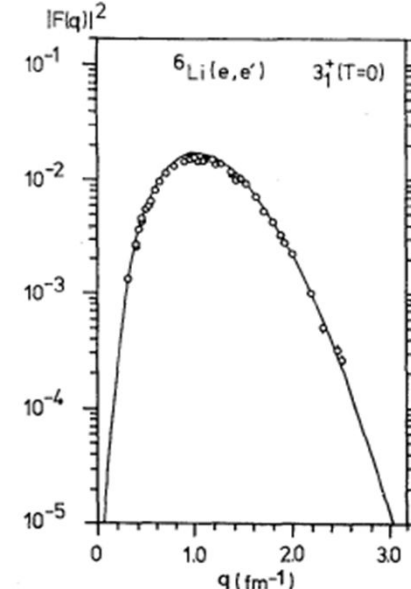
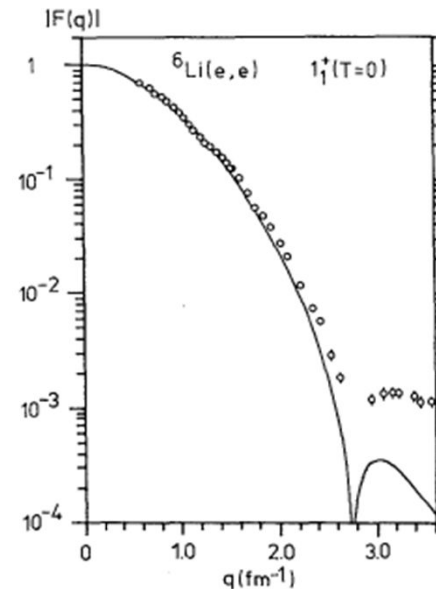
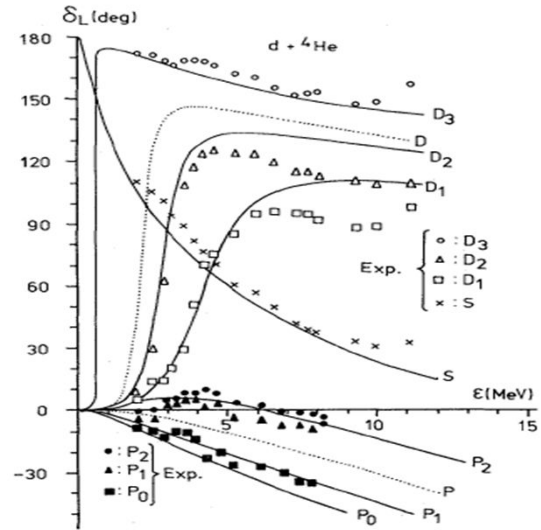
$$\Psi_{JM}(\vec{r}, \vec{R}) = \sum_L Y_{JM}^{\ell_0 I_0 L} \phi_0(r) \chi_{\ell_0 I_0 LJ}(P_0, R) / R + \sum_{\ell, I, L} Y_{JM}^{\ell I L} \int_0^{\infty} \phi_{\ell I}(k, r) \chi_{\ell I LJ}(P, R) / R dk,$$

After the discretization,

$$\Psi_{JM}^{CDCC}(\vec{r}, \vec{R}) = \sum_L Y_{JM}^{\ell_0 I_0 L} \phi_0(r) \hat{\chi}_{\gamma_0}(P_0, R) / R + \sum_{i=1}^N \sum_{\ell=0}^{\ell_{\max}} \sum_I \sum_L Y_{JM}^{\ell I L} \hat{\phi}_{i I}(r) \hat{\chi}_{\gamma}(P_{\gamma}, R) / R,$$

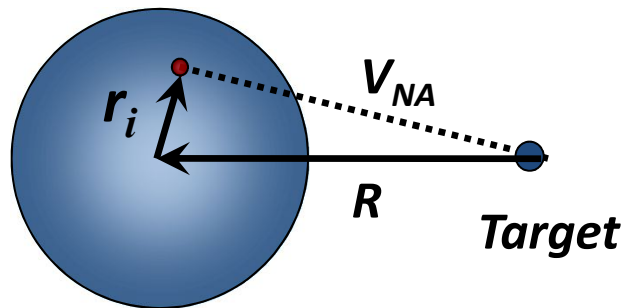
○ 核の微視的波動関数（例：CDCC $^{6,7}\text{Li}$ ）

scattering phase shifts & charge form factors の再現



○ 入射核--標的核間相互作用

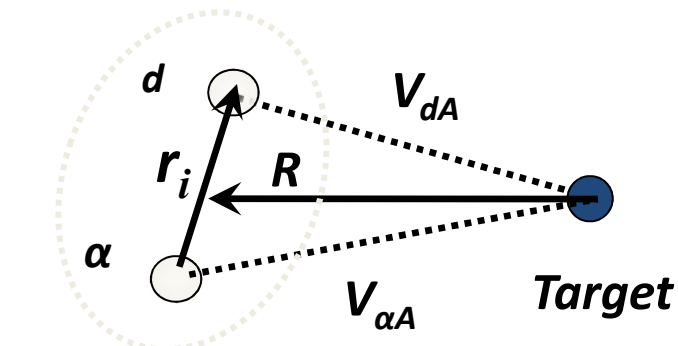
Single-Folding Model (SFM)



Projectile

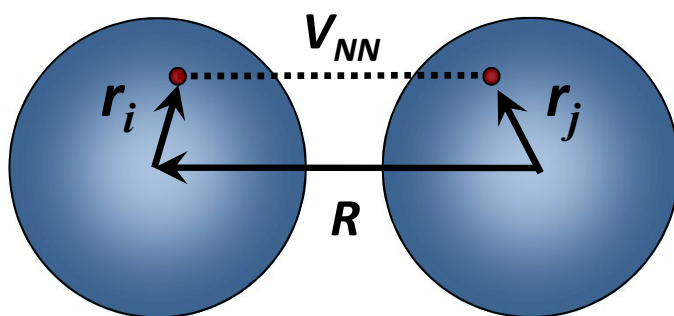
diagonal & coupling potentials

Cluster-Folding Model (CFM)



Projectile

Double-Folding Model (DFM)



Projectile

$$V_{SFM}(R) = \int \rho_p(\vec{r}_1) V_{NA}^{(opt)}(\vec{R} - \vec{r}_1) d\vec{r}_1$$

V_{NA} : N-核 optical potential

$$V_{CFM}(\vec{R}) = \langle \phi(\vec{r}) | V_{d-A}(\vec{R} + \frac{m_d}{M}\vec{r}) + V_{\alpha-A}(\vec{R} - \frac{m_\alpha}{M}\vec{r}) | \phi(\vec{r}) \rangle$$

V_{CA} : Cluster-核 optical potential

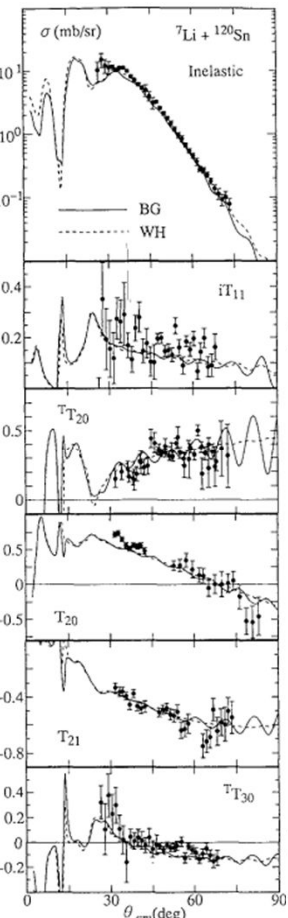
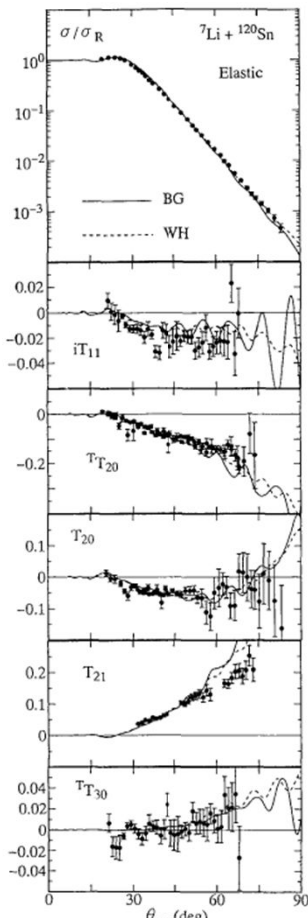
$$V_{DFM}(R) = \int \rho_p(\vec{r}_1) \rho_t(\vec{r}_2) v_{NN}(\vec{R} + \vec{r}_1 - \vec{r}_2) d\vec{r}_1 d\vec{r}_2$$

V_{NN} : effective N-N interaction (M3Y, DDM3Y, JLM)

$$\rho_{ik}(\vec{r}) = \langle \phi_i(\xi) | \sum_i \delta(\vec{r}_i - \vec{r}) | \phi_k(\xi) \rangle$$

○偏極量における folding potential type (SF, CF, DF)の違い CDCC

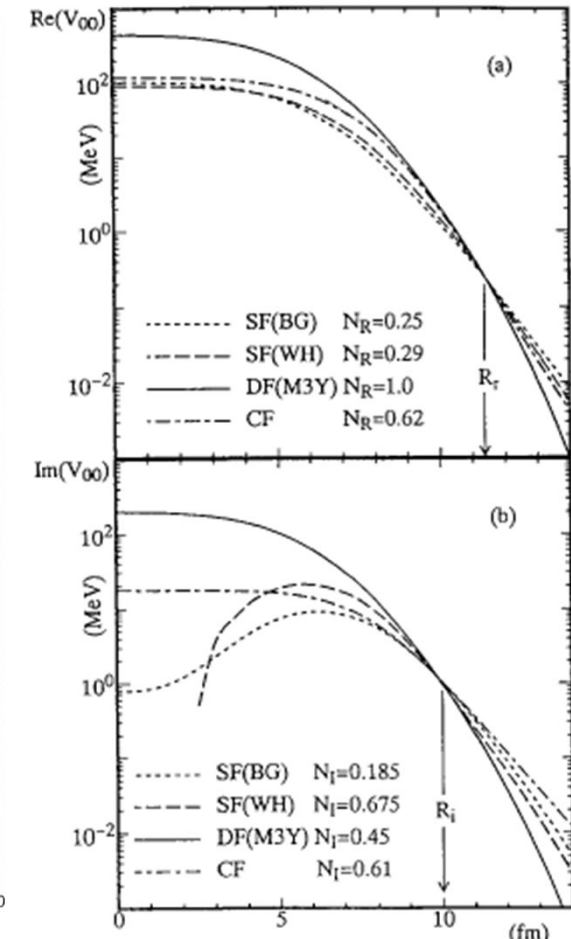
Y.H., Sakuragi, Tanifuji, PLB318 ('93) 32



SF

CF, DF

7Li + 120Sn, E(lab) = 44 MeV



diagonal part of SF, CF, DF pot.

○ Cluster Folding model の不具合（低エネルギー散乱） CDCC

Volume 258, number 1,2

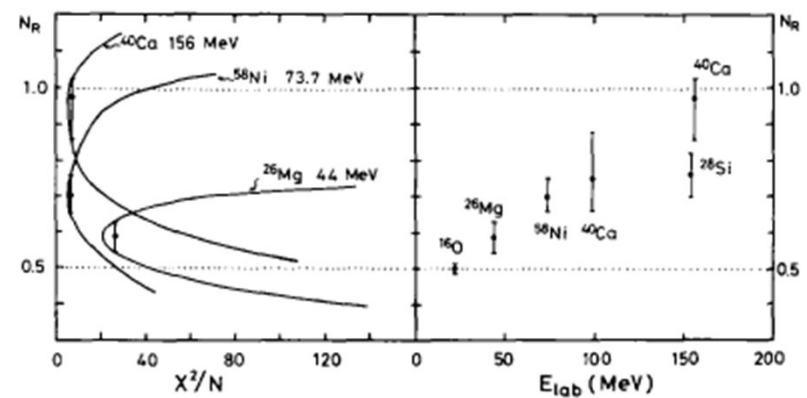
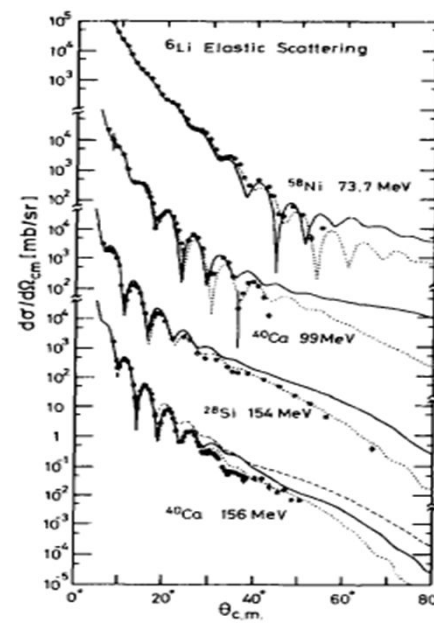
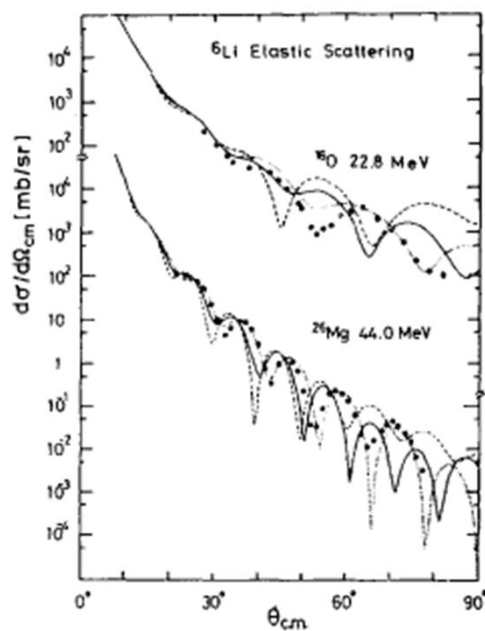
PHYSICS LETTERS B

4 April 1991

Anomalous renormalization of cluster-folding interactions for ${}^6\text{Li}$ -nucleus scattering at low energies

Y. Hirabayashi and Y. Sakuragi

Department of Physics, Osaka City University, Sumiyoshi-ku, Osaka 558, Japan

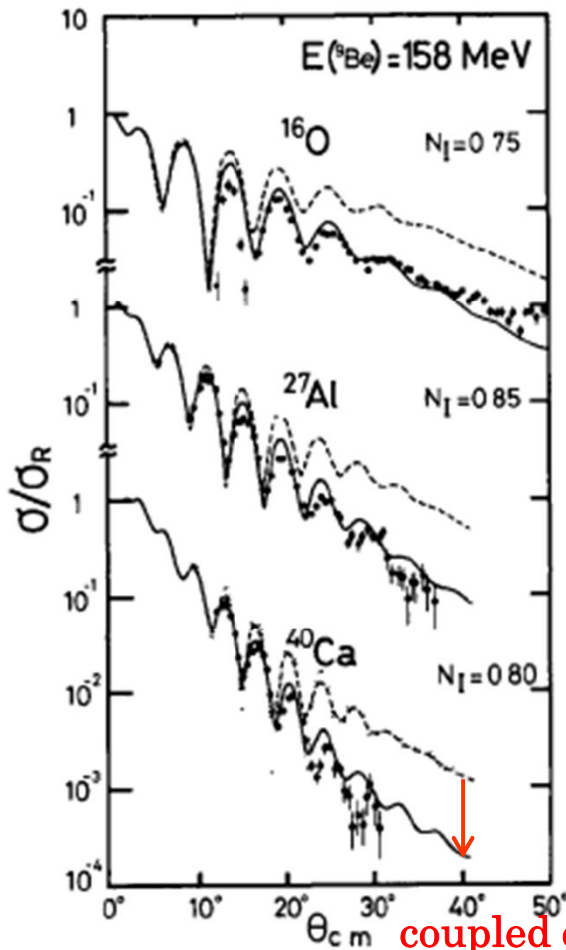


○ ${}^9\text{Be}$ 弹性散乱の角分布における分解過程の寄与と

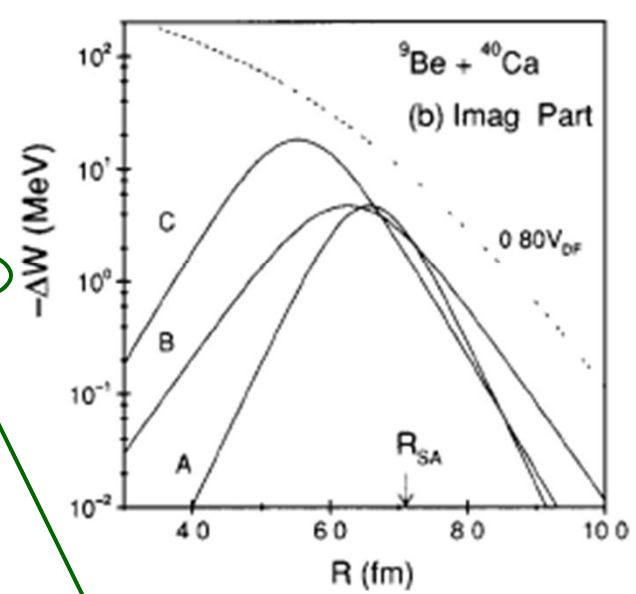
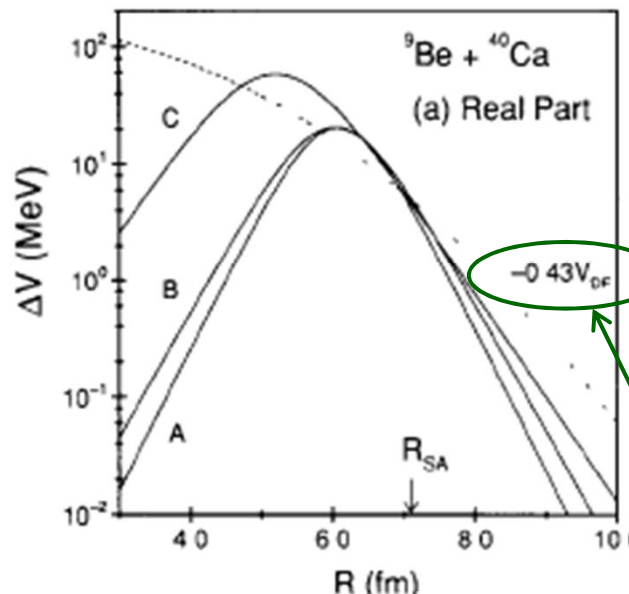
dynamical polarization (動的分極) potential

Microscopic CC

Y.H., Okabe, Sakuragi, PLB221 ('89) 227



coupled channel の効果
(分解過程の寄与)



$$V_{opt} = V_{00} + \sum_{\alpha, \alpha'} V_{0\alpha} \frac{1}{E - H_{QQ} + i\varepsilon} V_{\alpha'0}$$

dynamic polarization potential

取り入れなかった模型空間(Q)の寄与

◆ Double Folding Model と Dynamic Polarization Potential

FOLDING MODEL POTENTIALS FROM REALISTIC INTERACTIONS
FOR HEAVY-ION SCATTERING

Physics Reports 55(79) 183

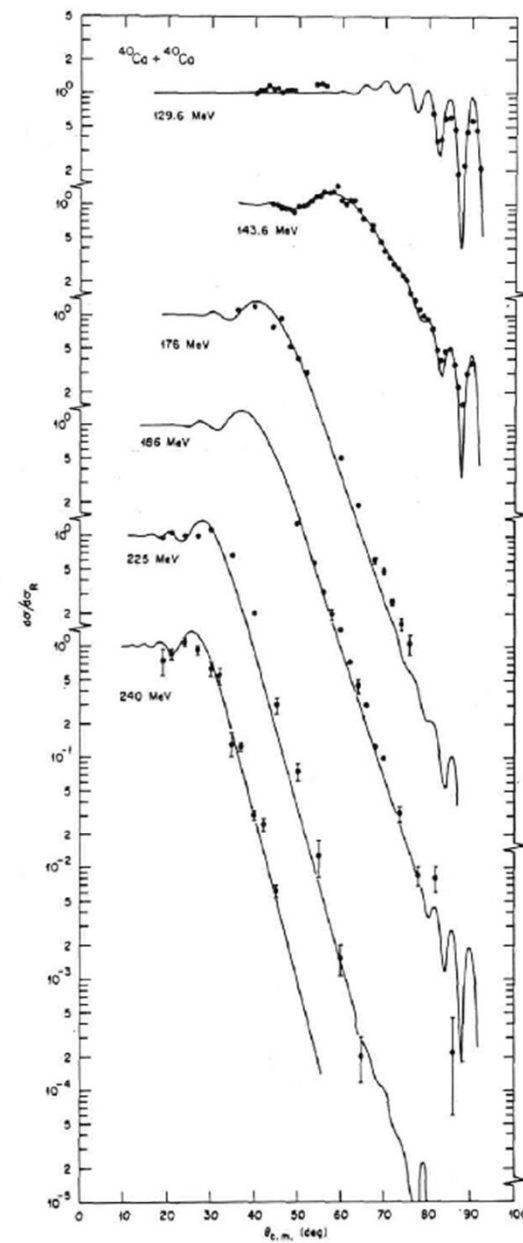
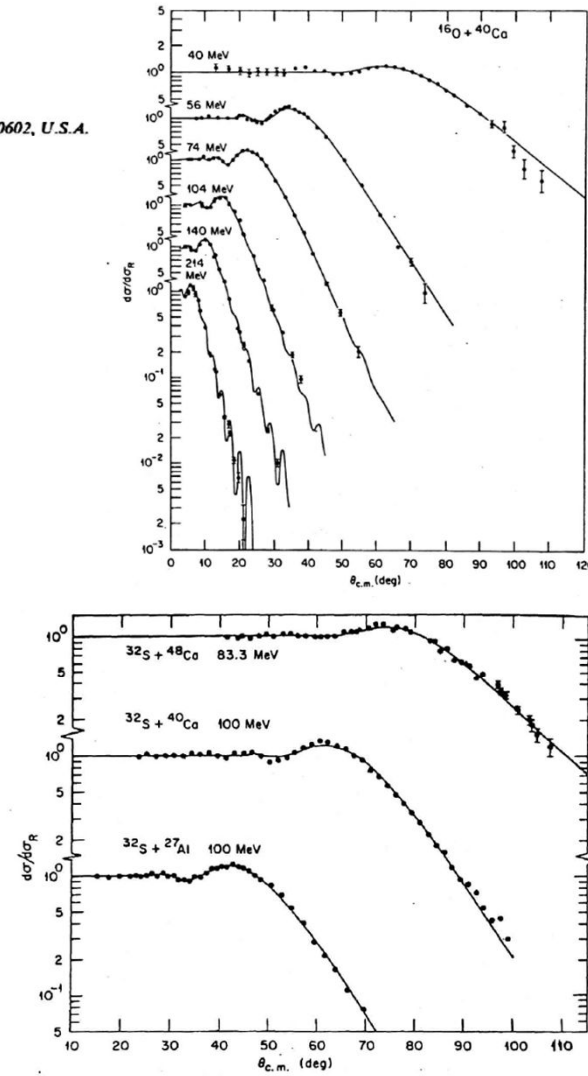
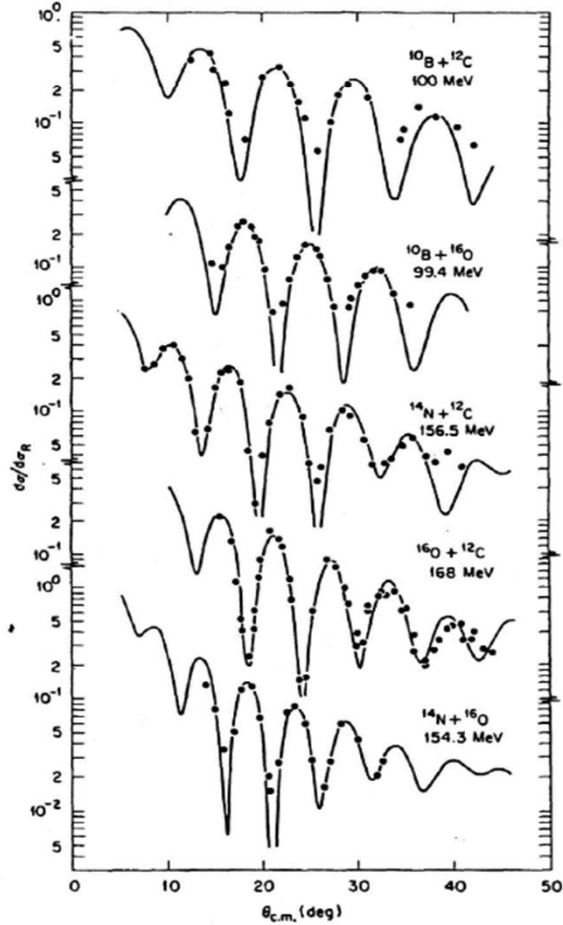
G.R. SATCHLER

Oak Ridge National Laboratory*, Oak Ridge, Tennessee 37830, U.S.A.

and

W.G. LOVE

Dept. of Physics and Astronomy, University of Georgia**, Athens, Georgia 30602, U.S.A.



System ^{a)}	E_{Lab} (MeV)	N	W (MeV)
$^{10}\text{B} + ^{12}\text{C}$	100	1.03	15.1
$^{10}\text{B} + ^{16}\text{O}$	99.4	1.04	16.5
$^{11}\text{B} + ^{208}\text{Pb}$	72.2	1.26	18.8
$^{11}\text{B} + ^{209}\text{Bi}$	74.6	1.45	20.7
$^{12}\text{C} + ^{12}\text{C}$	70–126	1.01–1.13	10–19
$^{12}\text{C} + ^{28}\text{Si}$	131.5	0.84	52.4
$^{12}\text{C} + ^{40}\text{Ca}$	45	1.14	10.4
$^{12}\text{C} + ^{90}\text{Zr}$	98	0.98	8.9
$^{12}\text{C} + ^{142}\text{Nd}$	70.4	1.15	15.8
$^{12}\text{C} + ^{208}\text{Pb}$	96	1.25	16.0
$^{12}\text{C} + ^{208}\text{Pb}$	116.4	1.26	14.7
$^{13}\text{C} + ^{207}\text{Pb}$	86.1	1.27	31.6
$^{14}\text{N} + ^{12}\text{C}$	156.5	1.03	15.1
$^{14}\text{N} + ^{16}\text{O}$	154.3	1.30	18.3
$^{15}\text{N} + ^{89}\text{Y}$	49.5	1.18	15.1
$^{16}\text{O} + ^{12}\text{C}$	168	1.11	18.0
$^{16}\text{O} + ^{28}\text{Si}$	37.7	1.01	7.5
$^{16}\text{O} + ^{28}\text{Si}$	53	1.00	8.5
$^{16}\text{O} + ^{28}\text{Si}$	60	1.01	8.5
$^{16}\text{O} + ^{28}\text{Si}$	66	1.01	7.3
$^{16}\text{O} + ^{28}\text{Si}$	72	1.00	9.1
$^{16}\text{O} + ^{28}\text{Si}$	81	1.00	8.6
$^{16}\text{O} + ^{28}\text{Si}$	141.5	0.91	74.3
$^{16}\text{O} + ^{28}\text{Si}$	215.2	0.76	79.0
$^{16}\text{O} + ^{40}\text{Ca}$	40	1.14	12.9
$^{16}\text{O} + ^{40}\text{Ca}$	55.6	1.27	12.9
$^{16}\text{O} + ^{40}\text{Ca}$	60	1.26	13.3
$^{16}\text{O} + ^{40}\text{Ca}$	74.4	1.14	12.9
$^{16}\text{O} + ^{40}\text{Ca}$	103.6	0.99	13.2
$^{16}\text{O} + ^{40}\text{Ca}$	139.6	1.23	14.7
$^{16}\text{O} + ^{40}\text{Ca}$	214.1	1.05	13.8
$^{16}\text{O} + ^{40}\text{Ca}$	40	0.98	13.3
$^{16}\text{O} + ^{40}\text{Ca}$	56	0.98	13.3
$^{16}\text{O} + ^{59}\text{Co}$	40	0.98	12.4
$^{16}\text{O} + ^{59}\text{Co}$	45.5	0.87	11.1
$^{16}\text{O} + ^{59}\text{Co}$	49	1.10	10.3
$^{16}\text{O} + ^{59}\text{Co}$	52	0.99	12.0
$^{16}\text{O} + ^{59}\text{Co}$	56	1.00	12.2
$^{16}\text{O} + ^{59}\text{Co}$	141.7	1.00	11.7

System ^{a)}	E_{Lab} (MeV)	N	W (MeV)
$^{16}\text{O} + ^{60}\text{Ni}$	61.4	1.04	10.8
$^{16}\text{O} + ^{60}\text{Ni}$	141.7	1.00	10.7
$^{16}\text{O} + ^{88}\text{Sr}$	48	1.36	10.4
$^{16}\text{O} + ^{88}\text{Sr}$	52	1.19	11.6
$^{16}\text{O} + ^{88}\text{Sr}$	56	1.21	19.8
$^{16}\text{O} + ^{88}\text{Sr}$	59	1.22	23.6
$^{16}\text{O} + ^{208}\text{Pb}$	129.5	1.16	19.4
$^{16}\text{O} + ^{208}\text{Pb}$	192	0.95	15.6
$^{16}\text{O} + ^{208}\text{Pb}$	312.6	1.05	11.4
$^{17}\text{O} + ^{40}\text{Ca}$	61.07	1.10	13.9
$^{32}\text{S} + ^{27}\text{Al}$	100	1.08	24.5
$^{32}\text{S} + ^{32}\text{S}$	90.88	1.22	22.7
$^{32}\text{S} + ^{40}\text{Ca}$	100	1.26	24.4
$^{32}\text{S} + ^{48}\text{Ca}$	83.3	1.09	58.7
$^{40}\text{Ca} + ^{40}\text{Ca}$	143.6	1.32	14.7
$^{40}\text{Ca} + ^{40}\text{Ca}$	129.6	1.32	14.7
$^{40}\text{Ca} + ^{40}\text{Ca}$	176.0	1.32	14.7
$^{40}\text{Ca} + ^{40}\text{Ca}$	186.0	1.32	14.7
$^{40}\text{Ca} + ^{40}\text{Ca}$	225	1.32	14.7
$^{40}\text{Ca} + ^{40}\text{Ca}$	240	1.32	14.7

System	E_{Lab} (MeV)	N	W (MeV)
^6Li Scattering			
$^6\text{Li} + ^{28}\text{Si}$	135.1	0.62	43.5
$^6\text{Li} + ^{40}\text{Ca}$	28	0.62	9.8
$^6\text{Li} + ^{40}\text{Ca}$	30	0.60	9.5
$^6\text{Li} + ^{40}\text{Ca}$	34	0.60	10.2
$^6\text{Li} + ^{40}\text{Ca}$	50.6	0.63	11.3
$^6\text{Li} + ^{40}\text{Ca}$	156	0.66	30.6
$^6\text{Li} + ^{44}\text{Ca}$	30	0.55	11.2
$^6\text{Li} + ^{48}\text{Ca}$	28	0.65	11.5
$^6\text{Li} + ^{48}\text{Ca}$	34	0.60	9.6
$^6\text{Li} + ^{58}\text{Ni}$	22.8	0.37	11.1
$^6\text{Li} + ^{58}\text{Ni}$	50.6	0.60	11.9
$^6\text{Li} + ^{90}\text{Zr}$	34	0.79	11.8
$^6\text{Li} + ^{90}\text{Zr}$	73.7	0.58	13.4
$^6\text{Li} + ^{90}\text{Zr}$	156	0.63	27.1
$^6\text{Li} + ^{124}\text{Sn}$	50.6	0.78	12.3
$^6\text{Li} + ^{208}\text{Pb}$	50.6	0.59	11.8

^9Be scattering

Target	E_{Lab} (MeV)	N	W (MeV)
^{28}Si	12		
	14		
	17		
	20		
	23		
	26		
	30		
	50 ± 1	0.42	9.7
	121	0.55	20.9
	201.6	0.49	22.2
^{40}Ca	14		
	20		
	26		
	34	0.34	12.3
^{58}Ni	20		
	26	0.62	13.3
^{208}Pb	50 ± 1	0.36	14.0

Love & Satchler,
Physics Reports 55('79) 183

○ ${}^6\text{Li}$ 散乱偏極量における分解状態の寄与と模型空間に対する収束性

CDCC

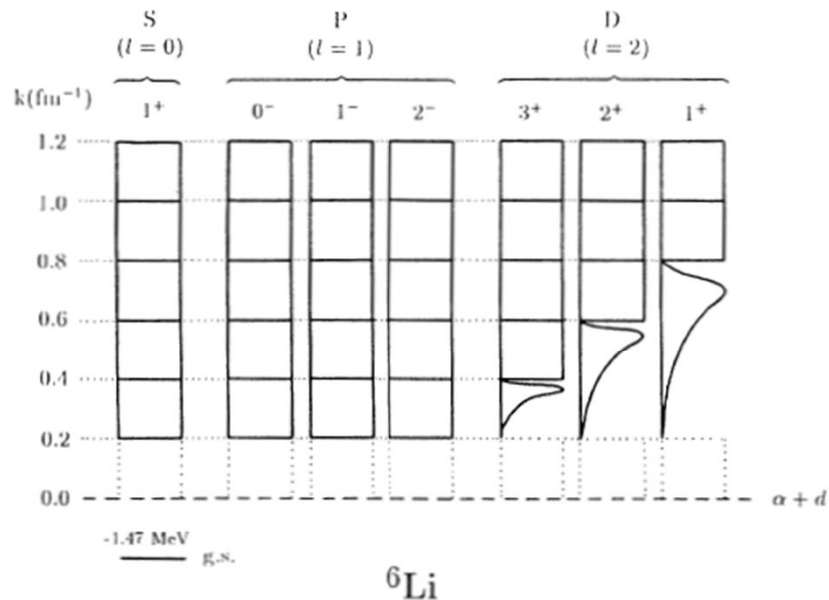
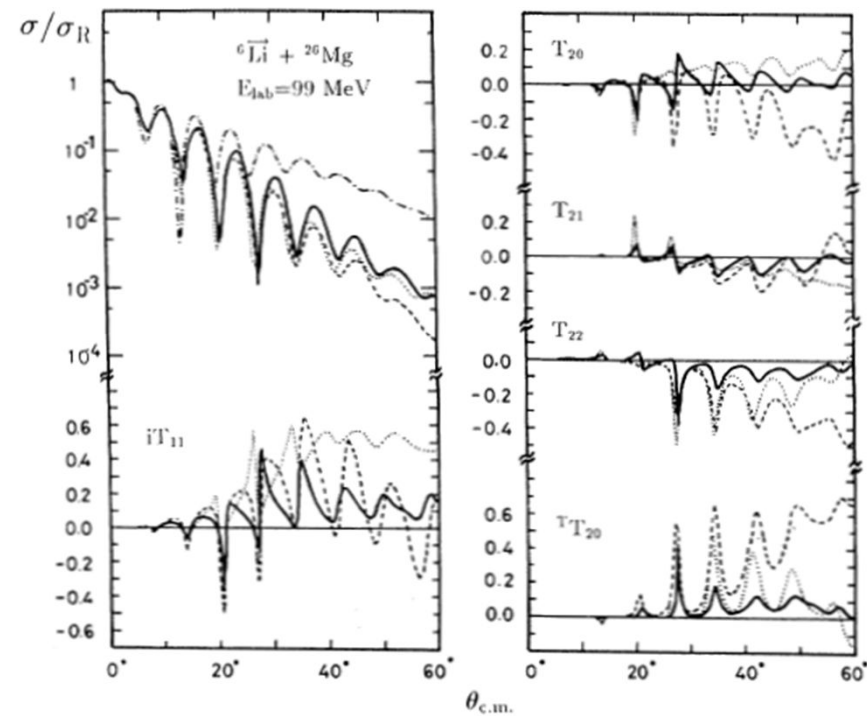


FIG. 3. The full model space of ${}^6\text{Li} \rightarrow \alpha + d$ breakup states resulting from the tests of convergence.

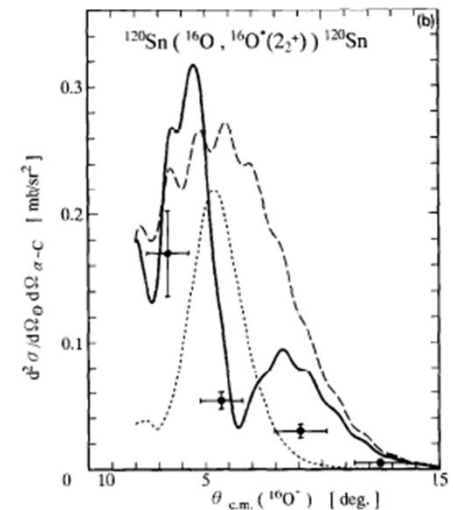
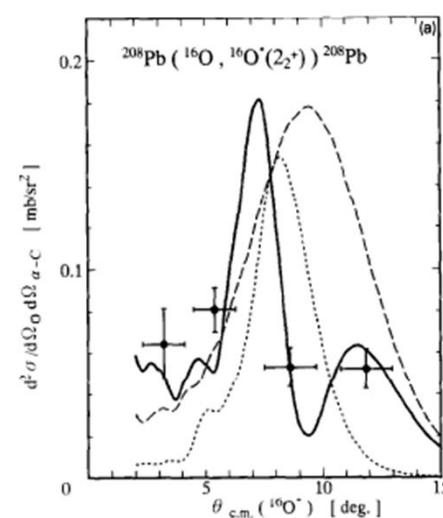
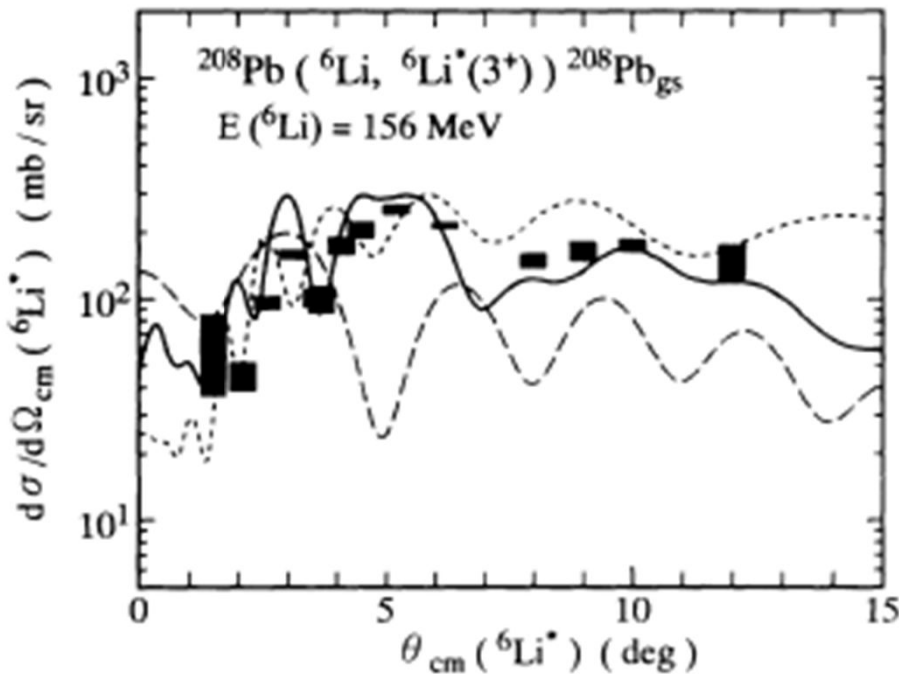


Y.H., PRC44(91) 1581

○ Astrophysical Interest (Coulomb breakup or Nuclear Breakup ?)

CDCC, MCC

Y.H., Sakuragi, PRL69(92) 1892



O'Kelly et.al.(Y.H.), PLB393(97) 301

- Nuclear/Coulomb breakup の定量的記述の成功
- 強い Nuclear breakup (超前方でさえ)
→ Coulomb breakup シナリオの破綻

○ $^{24}\text{Mg} = ^{12}\text{C}^* + ^{12}\text{C}^*$ 高励起状態の構造

Microscopic CC

68, NUMBER 9

PHYSICAL REVIEW LETTERS

2 M

Evidence for Alpha-Particle Chain Configurations in ^{24}Mg

A. H. Wuosmaa, R. R. Betts, B. B. Back, M. Freer, B. G. Glagola, Th. Happ, D. J. Henderson,
and P. Wilt

Physics Division, Argonne National Laboratory, Argonne, Illinois 60439

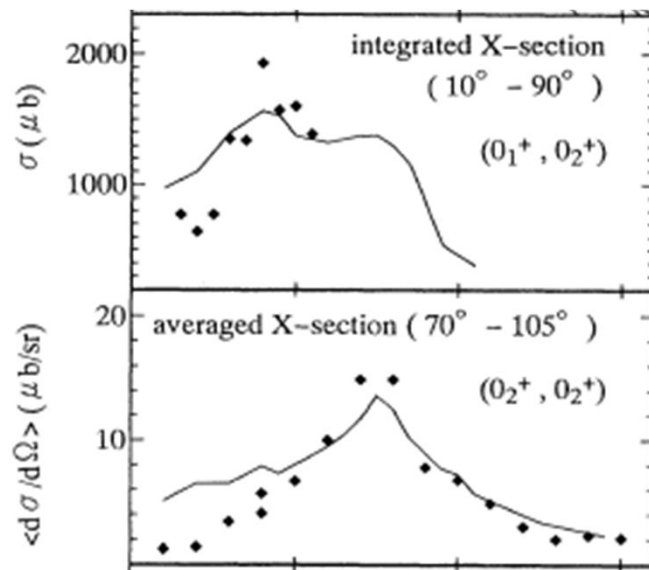
I. G. Bearden

Physics Department, Purdue University, West Lafayette, Indiana 47907

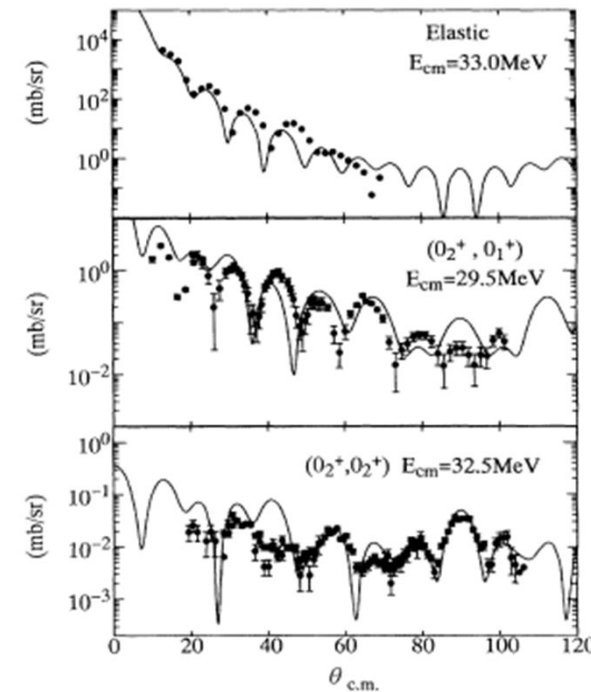
$^{24}\text{Mg} = ^{12}\text{C}(0_2^+) + ^{12}\text{C}(0_2^+)$, $E_{\text{cm}}=32.5\text{MeV}$ の共鳴は 6 α 鎖状構造か?

$^{12}\text{C} (^{12}\text{C}, ^{12}\text{C}(0_2^+)) ^{12}\text{C}(0_2^+)$

Y.H., Sakuragi, Abe, PRL74('95) 4141

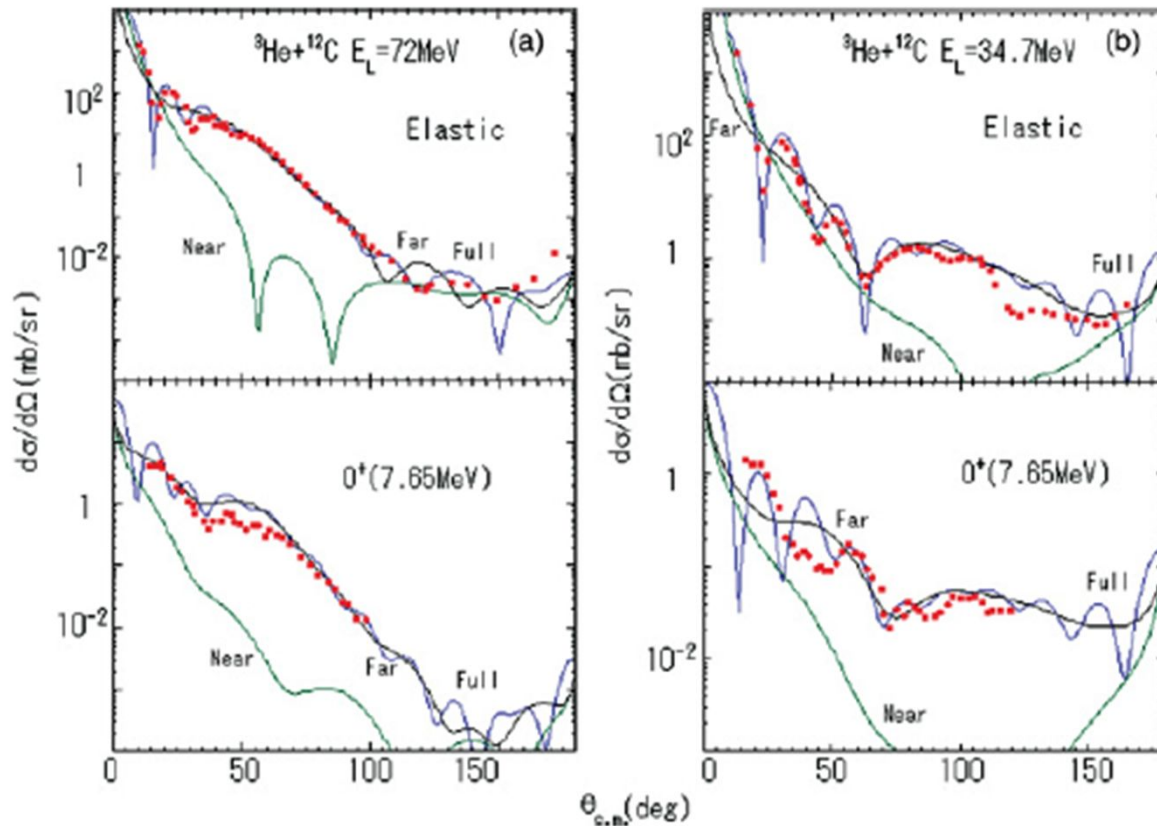


→ 2 つの $^{12}\text{C}(0_2^+) = 3\alpha$ (非鎖状) の弱結合状態



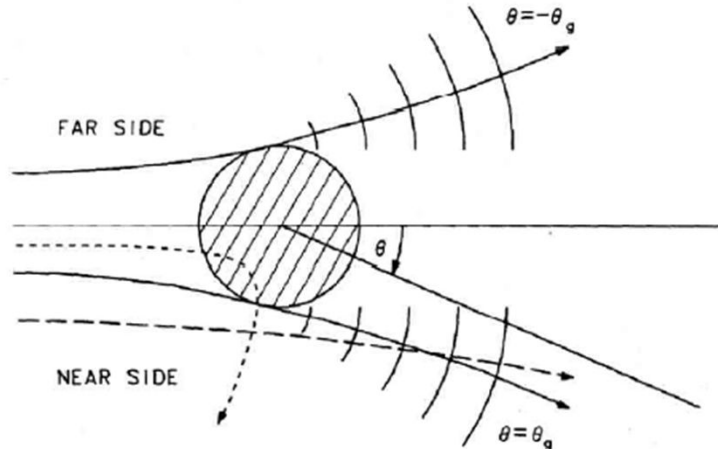
○ $^{12}\text{C}(0_2^+)$ Hoyle state (α 凝縮状態?) と核虹 MCC

Ohkubo, Y.H., PRC75 ('07) 3044609

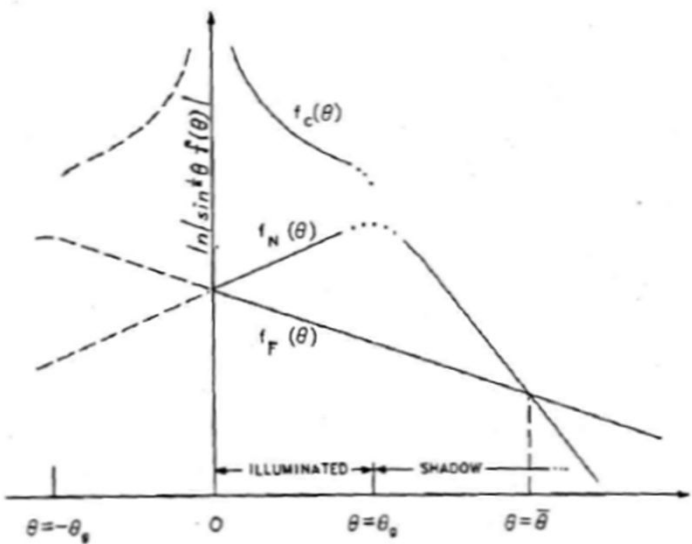


- 核虹の存在
- 弹性散乱とHoyle state における位置（角度）の違い

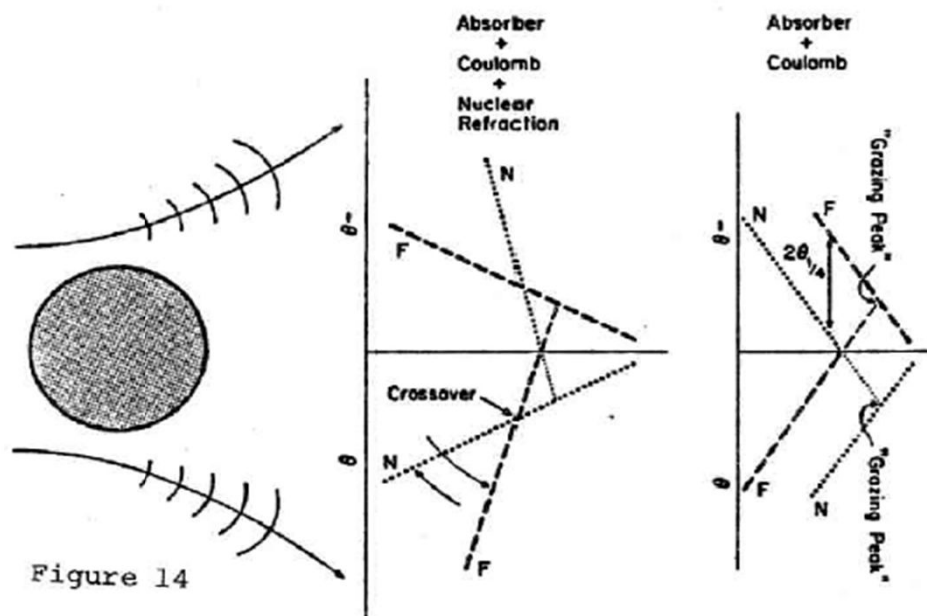
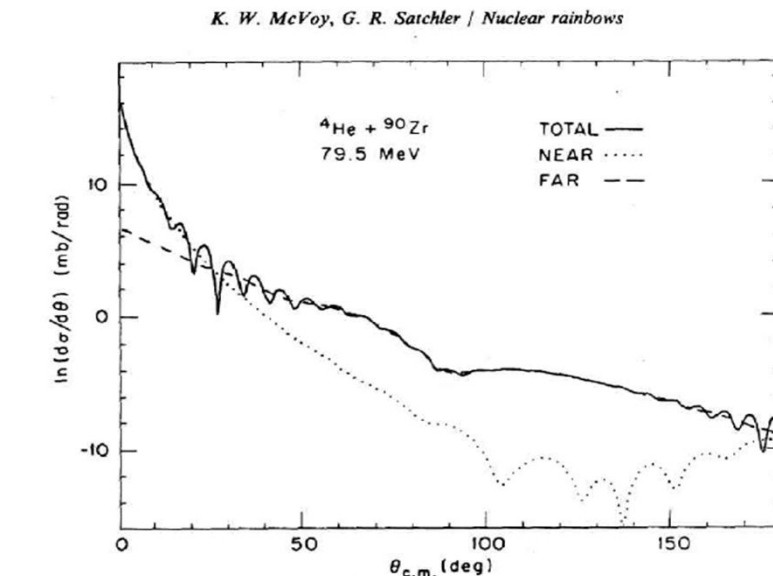
◆ Near/Far decomposition



K. W. McVoy, G. R. Satchler / Nuclear rainbows



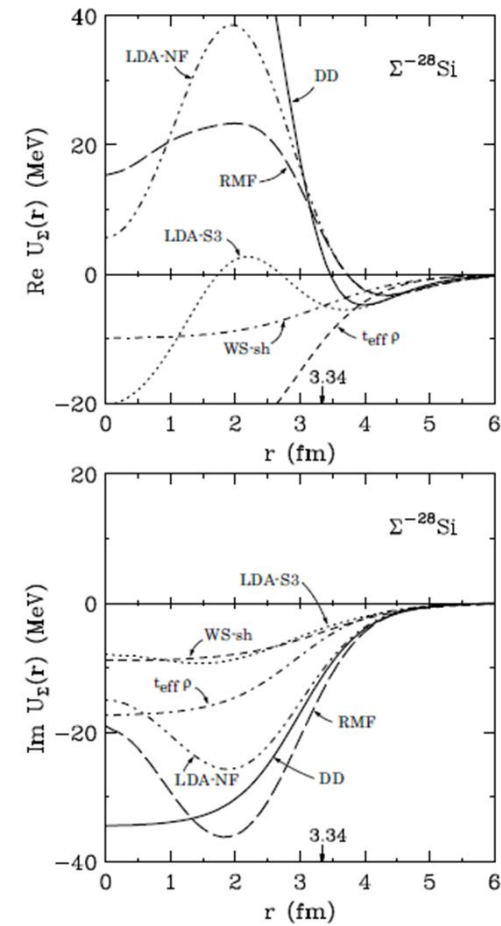
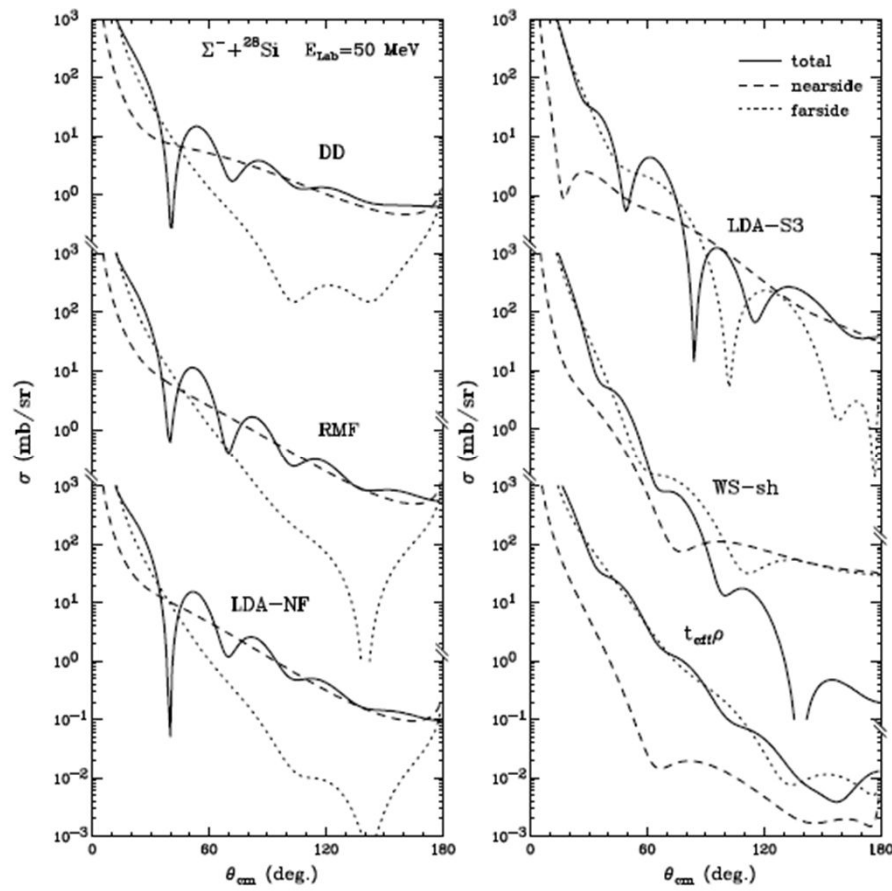
McVOY & Satchler, NPA417(84) 157



McVOY, Lecture Note of 1983 RCNP KIKUCHI Summer School

○ Σ^- + 原子核散乱微分断面積

potential scattering (single channel)



- Near/Far 逆転 (\leftrightarrow 原子核+原子核散乱)
- 十分な斥力ポテンシャル
- 斥力部分と引力部分 (Coulomb含む) の競合による角分布

○ ${}^3\text{He}$ (K^- , $\pi^{-/+}$) reactions

